

## Accessing transversity with interference fragmentation functions

Marco Radici

*Dipartimento di Fisica Nucleare e Teorica, Università di Pavia, I-27100 Pavia, Italy  
and Istituto Nazionale di Fisica Nucleare, Sezione di Pavia, I-27100 Pavia, Italy*

Rainer Jakob

*Fachbereich Physik, Universität Wuppertal, D-42097 Wuppertal, Germany*

Andrea Bianconi

*Dipartimento di Chimica e Fisica per i Materiali e per l'Ingegneria, Università di Brescia, I-25133 Brescia, Italy*

(Received 19 October 2001; published 1 April 2002)

We discuss in detail the option to access the transversity distribution function  $h_1(x)$  by utilizing the analyzing power of interference fragmentation functions in two-pion production inside the same current jet. The transverse polarization of the fragmenting quark is related to the transverse component of the relative momentum of the hadron pair via a new azimuthal angle. As a specific example, we spell out thoroughly the way to extract  $h_1(x)$  from a measured single spin asymmetry in two-pion inclusive lepton-nucleon scattering. To estimate the sizes of observable effects we employ a spectator model for the fragmentation functions. The resulting asymmetry of our example is discussed as arising in different scenarios for the transversity.

DOI: 10.1103/PhysRevD.65.074031

PACS number(s): 13.60.Hb, 12.38.Lg, 13.85.Ni, 13.87.Fh

### I. INTRODUCTION

At leading power in the hard scale  $Q$ , the quark content of a nucleon state is completely characterized by three distribution functions (DF). They describe the quark momentum and spin with respect to a preferred longitudinal direction induced by a hard scattering process. Two of them, the momentum distribution  $f_1$  and the longitudinal spin distribution  $g_1$ , have been reliably extracted from experiments and accurately parametrized. Their knowledge has deeply contributed to the studies of the quark-gluon substructure of the nucleon. The third one, the transversity distribution  $h_1$ , measures the probability difference to find the quark polarization parallel versus antiparallel to the transverse polarization of a nucleon target. Therefore, it is nondiagonal on the helicity basis [1]; since helicity and chirality coincide up to quark mass corrections, it is usually referred to as a “chiral-odd” function. Hard scattering processes in QCD preserve helicity; hence, the  $h_1$  is difficult to measure and is systematically suppressed like  $\mathcal{O}(1/Q)$ , for example, in inclusive deep inelastic scattering (DIS) [1]. A chiral-odd partner is needed that counterbalances the helicity flip with some soft physics process in order to filter the transversity out of the cross section.

Historically, the so-called double spin asymmetry (DSA) in Drell-Yan processes with two transversely polarized protons ( $p^\uparrow$ ) was suggested first [2]. However, the transversity distribution  $h_1$  for antiquarks in the proton is presumably small [3]. Moreover, an upper limit for the DSA derived in a next-to-leading order analysis by using the Soffer bounds on transversity was found to be discouragingly low [4].

Alternative ways have been discussed about DIS (for a review, see Refs. [3,1]), which all imply semi-inclusive reactions in order to provide the chiral-odd partner to  $h_1$ . In fact, in this case new functions enter the game, the fragmentation functions (FF), which give information on the hadronic structure complementary to the one delivered by the DF. At

leading twist, the FF describe the hadron content of quarks and, more generally, they contain information on the hadronization process leading to the detected hadrons; as such, they give information also on the quark content of hadrons that are not (or even do not exist as) stable targets. The FF are also universal, but are presently less known than the DF because a very high resolution and/or acceptance and a good particle identification are required in the detection of the final state.

All suggested proposals for extracting  $h_1$  are usually based on spin asymmetry measurements, where at least two more meaningful independent vectors are required with respect to the corresponding unpolarized process. We already mentioned the DSA, where two of these vectors are represented by the polarizations of two initial (Drell-Yan), or one initial and one final (DIS), hadrons. There are also single spin asymmetries (SSA) in semi-inclusive reactions, where the polarization of the hadron target is accompanied by a relevant transverse vector describing the noncollinear dynamics of a detected final unpolarized hadron system.

The most famous example is the Collins effect [5] in reactions like semi-inclusive  $ep^\uparrow \rightarrow e' \pi X$ , or  $p^\uparrow p \rightarrow \pi X$ , where the single leading pion is detected not collinearly with the associated jet. The analyzing power of the transverse polarization of the fragmenting quark is represented by the transverse component of the momentum of the detected hadron with respect to the current jet axis. At leading twist,  $h_1$  can be extracted through a moment of the so-called Collins function  $H_1^\perp$ , the prototype of a new class of FF, the interference FF, which are not only chiral-odd, but also *naive* time-reversal odd (for brevity, *T*-odd): in the absence of two or more interfering reaction channels with a significant relative phase, the FF can be interpreted as the decay probability of a quark and, consequently, they are forbidden by time-reversal invariance [6–8].

Similarly, *T*-odd interference FF show up also when the

final hadronic system is represented by two unpolarized leading hadrons inside the same current jet [9–11]. In a previous work, we have discussed the general framework and the general properties of such interference FF arising at leading twist in this case [12]. The richer structure of the cross section offers new possibilities. In Sec. II of this paper, we detail the model-independent strategy for extracting  $h_1$  from the cross section at leading twist. For the test case of a semi-inclusive lepton-nucleon DIS, it is shown that a SSA can also be built by identifying the pair of relevant vectors with the transverse polarization of the target and with the transverse component of the relative momentum of the hadron pair, irrespectively of the noncollinearity of each individual hadron. Assuming that the residual interactions between each leading hadron and the undetected jet are of higher order than the one between the two hadrons themselves, the main result is that  $h_1$  can be factorized from the leading-twist cross section together with a novel interference FF,  $H_1^*$ . This new analyzing power,  $H_1^*$ , filters out the  $h_1$  in a very advantageous way. The asymmetry is related to just one azimuthal angle, while its independence from the noncollinearity of each hadron implies that collinear factorization holds; at variance with the case of the Collins effect, this leads to an exact cancellation of all collinear divergences, and, in principle, it could make the evolution equations simpler [13].

From the experimental point of view, for the semi-inclusive deep-inelastic electro-production of single pions only one observation of a nonvanishing SSA has been reported [14], while no corresponding ones for two pion production are yet known to us. This implies that it is presently impossible to deduce a reasonable parametrization of interference FF beyond the “simple” chiral-even decay probability  $D_1$  [15]. Nevertheless, it would be highly desirable to have a quantitative estimate of these FF, in order to explore if the proposed SSA are nonvanishing and actually measurable. For this reason, model calculations were performed, particularly in the context of the so-called spectator approximation [16,17], and specifically also about the Collins effect [18]. In this approach, stringent constraints are put on the representation of the spectator jet, which allow for a drastic simplification of the calculations. The key ingredients are vertex form factors, which represent the interface between the elementary hard scattering with the external probe and the soft processes included in the fragmentation by ensuring a proper behavior of the FF (and DF) in the asymptotic limits. The necessary parameters are fixed by comparing sum rules and moments of such functions with available parametrizations and/or experimental data. A successful description of the available quark distribution functions and of the unpolarized quark fragmentation function  $D_1$  has been achieved [17], so that the model can be considered as a reasonable and useful testing ground for further explorations.

In a previous work, we have extended the spectator approximation to the calculation of interference FF for the case of a leading proton-pion pair inside the same jet and with invariant mass close to the Roper resonance [19]. Here, in Sec. III we repeat the calculation for the experimentally more relevant case of a  $\pi^+\pi^-$  pair produced with invariant mass

close to the  $\rho$  resonance in a semi-inclusive lepton-nucleon DIS. Because of the total unavailability of experimental data, some of the parameters are fixed in a rather arbitrary way, but the related uncertainty is tentatively discussed. Therefore, the results, discussed in Sec. IV, should not be interpreted as a precise prediction, but rather as an example of how the reasonably assumed simple processes can indeed lead to nonvanishing interference FF and SSA; they also represent a useful tool to explore the measurability of such SSA and, consequently, the actual possibility for extracting  $h_1$  from them. This information should be pertinent, for instance, to HERMES (when the transversely polarized target will be operative) or even better at COMPASS (because of higher counting rates); it will also be very interesting for the future options in hadronic physics such as ELFE, DESY TESLA-N and EIC. In addition, if factorization holds, our results could be useful also for the spin physics program at the BNL Relativistic Heavy Ion Collider (RHIC), where the extraction of transversity is planned via a SSA in  $p-p$  reactions.

Finally, in Sec. V conclusions and outlooks are given.

## II. SINGLE SPIN ASYMMETRY FOR TWO HADRON-INCLUSIVE LEPTON-NUCLEON DIS

In this section we discuss the general properties of two-hadron interference FF when the kinematics is specialized to semi-inclusive DIS, and for this process we work out the formula for a SSA that isolates the transversity at leading twist. However, we emphasize that under the assumption of factorization the soft parts of the process, i.e. the DF and the interference FF, are universal objects and, therefore, the results can be generalized to other hard processes, such as proton-proton scattering.

### A. Interference fragmentation functions in semi-inclusive DIS

At leading order, the hadron tensor for two unpolarized hadron-inclusive lepton-nucleon DIS reads [12]

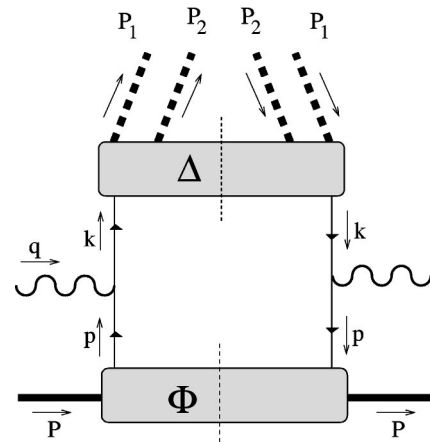


FIG. 1. Quark diagram contributing in leading order to two-hadron inclusive DIS when both hadrons are in the same quark current jet. There is a similar diagram for anti-quarks.

$$\begin{aligned}
2M\mathcal{W}^{\mu\nu} = & \int d p^- d k^+ d^2 \vec{p}_T d^2 \vec{k}_T \delta^2(\vec{p}_T + \vec{q}_T - \vec{k}_T) \\
& \times \text{Tr}[\Phi(p; P, S) \gamma^\mu \Delta(k; P_1, P_2) \gamma^\nu] \Big|_{k^- = P_h^- / z}^{p^+ = x P^+} \\
& + \begin{pmatrix} q \leftrightarrow -q \\ \mu \leftrightarrow \nu \end{pmatrix}, \quad (1)
\end{aligned}$$

where  $M$  is the target mass. The kinematics, also depicted in Fig. 1, represents a nucleon with momentum  $P(P^2 = M^2)$  and a virtual hard photon with momentum  $q$  that hits a quark carrying a fraction  $p^+ = x P^+$  of the parent hadron momentum. We describe a 4-vector  $a$  as  $[a^-, a^+, \vec{a}_T]$ , in terms of its

light-cone components  $a^\pm = (a^0 \pm a^3) / \sqrt{2}$  and a transverse bidimensional vector  $\vec{a}_T$ , such that for two 4-vectors  $a, b$  we have  $a \cdot b = a^+ b^- + a^- b^+ - \vec{a}_T \cdot \vec{b}_T$ . Because of momentum conservation in the hard vertex, the scattered quark has momentum  $k = p + q$ , and it fragments into two unpolarized hadrons, which carry a fraction  $(P_1 + P_2)^- \equiv P_h^- = z k^-$  of the ‘‘parent quark’’ momentum, and the rest of the jet.

The quark-quark correlator  $\Phi$  describes the nonperturbative processes that make the parton  $p$  emerge from the spin-1/2 target, and it is symbolized by the lower shaded blob in Fig. 1. Using Lorentz invariance, Hermiticity and parity invariance, the partly integrated  $\Phi$  can be parametrized at leading twist in terms of DF as

$$\begin{aligned}
\Phi(x, \vec{p}_T) \equiv & \int d p^- \Phi(p; P, S) \Big|_{p^+ = x P^+} \\
= & \frac{1}{2} \left\{ f_1 \not{h}_+ + f_{1T}^\perp \epsilon_{\mu\nu\rho\sigma} \gamma^\mu \frac{n_+^\nu p_T^\rho S_T^\sigma}{M} - \left( \lambda g_{1L} + \frac{(\vec{p}_T \cdot \vec{S}_T)}{M} g_{1T} \right) \not{h}_+ \gamma_5 - h_{1T} i \sigma_{\mu\nu} \gamma_5 S_T^\mu n_+^\nu \right. \\
& \left. - \left( \lambda h_{1L}^\perp + \frac{(\vec{p}_T \cdot \vec{S}_T)}{M} h_{1T}^\perp \right) \frac{i \sigma_{\mu\nu} \gamma_5 p_T^\mu n_+^\nu}{M} + h_1^\perp \frac{\sigma_{\mu\nu} p_T^\mu n_+^\nu}{M} \right\}, \quad (2)
\end{aligned}$$

where  $n_\pm = \frac{1}{2} [1 \mp 1, 1 \pm 1, \vec{0}_T]$  are light-like vectors with  $n_\pm^2 = n_\mp^2 = 0$ ,  $n_+ \cdot n_- = 1$  and  $a^\pm = a \cdot n_\mp$ ; the DF depend on  $x, \vec{p}_T$  and the polarization state of the target is fully specified by the light-cone helicity  $\lambda = M S^+ / P^+$  and the transverse component  $\vec{S}_T$  of the target spin. Similarly, the correlator  $\Delta$ , symbolized by the upper shaded blob in Fig. 1, represents the fragmentation of the quark into the two detected hadrons and the rest of the current jet and can be parametrized as [12]

$$\begin{aligned}
\Delta \equiv & \frac{1}{4z} \int d k^+ \Delta(k; P_1, P_2) \Big|_{k^- = P_h^- / z} \\
= & \frac{1}{4} \left\{ D_1 \not{h}_- - G_1^\perp \frac{\epsilon_{\mu\nu\rho\sigma} \gamma^\mu n_-^\nu k_T^\rho R_T^\sigma}{M_1 M_2} \gamma_5 \right. \\
& \left. + H_1^\perp \frac{\sigma_{\mu\nu} R_T^\mu n_-^\nu}{M_1 + M_2} + H_1^\perp \frac{\sigma_{\mu\nu} k_T^\mu n_-^\nu}{M_1 + M_2} \right\}, \quad (3)
\end{aligned}$$

where  $R \equiv (P_1 - P_2) / 2$  is the relative momentum of the hadron pair.

For convenience, we will choose a frame where, besides  $\vec{P}_T = 0$ , we have also  $\vec{P}_{hT} = 0$ . By defining the light-cone momentum fraction  $\xi = P_1^- / P_h^-$ , we can parametrize the final-state momenta as

$$\begin{aligned}
k &= \left[ \frac{P_h^-}{z}, z \frac{k^2 + \vec{k}_T^2}{2 P_h^-}, \vec{k}_T \right], \\
P_1 &= \left[ \xi P_h^-, \frac{M_1^2 + \vec{R}_T^2}{2 \xi P_h^-}, \vec{R}_T \right], \\
P_2 &= \left[ (1 - \xi) P_h^-, \frac{M_2^2 + \vec{R}_T^2}{2(1 - \xi) P_h^-}, -\vec{R}_T \right].
\end{aligned} \quad (4)$$

From the definition of the invariant mass of the hadron pair, i.e.  $M_h^2 \equiv P_h^2 = 2 P_h^+ P_h^-$ , and the on-shell condition for the two hadrons themselves,  $P_1^2 = M_1^2, P_2^2 = M_2^2$ , we deduce the relation

$$\vec{R}_T^2 = \xi(1 - \xi) M_h^2 - (1 - \xi) M_1^2 - \xi M_2^2 \quad (5)$$

which in turn puts a constraint on the invariant mass from the positivity requirement  $\vec{R}_T^2 \geq 0$ :

$$M_h^2 \geq \frac{M_1^2}{\xi} + \frac{M_2^2}{1 - \xi}. \quad (6)$$

After having given all the details of the kinematics, we can specify the actual dependence of the quark-quark correlator  $\Delta$  and of the FF. From the frame choice  $\vec{P}_{hT} = 0$ , the on-shell condition for both hadrons, Eq. (5), the constraint on

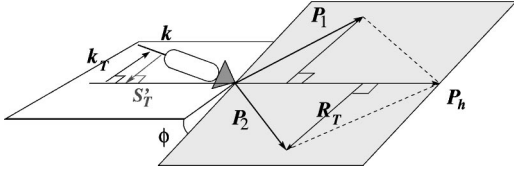


FIG. 2. The kinematics for the final state where a quark fragments into two leading hadrons inside the same current jet.

$k^-$  and the integration over  $k^+$  implied by the definition of  $\Delta$  in Eq. (3), we deduce that the actual number of independent components of the three 4-vectors  $k, P_1, P_2$  is five (cf. [12]). They can conveniently be chosen as the fraction of quark momentum carried by the hadron pair,  $z$ , the subfraction in which this momentum is further shared inside the pair,  $\xi$ , and the ‘‘geometry’’ of the pair in the momentum space, namely, the ‘‘opening’’ of the pair momenta,  $\vec{R}_T^2$ , the relative position of the jet axis and the hadron pair axis,  $\vec{k}_T^2$ , and the relative position of hadron pair plane and the plane formed by the jet axis and the hadron pair axis,  $\vec{k}_T \cdot \vec{R}_T$  (see Fig. 2).

Both DF and FF can be deduced from suitable projections of the corresponding quark-quark correlators. In particular, by defining

$$\begin{aligned} \Delta^{[\Gamma]}(z, \xi, \vec{k}_T^2, \vec{R}_T^2, \vec{k}_T \cdot \vec{R}_T) \\ \equiv \frac{1}{4z} \int d k^+ \text{Tr}[\Gamma \Delta(k, P_1, P_2)]|_{k^- = P_h^-/z}, \end{aligned} \quad (7)$$

we can deduce, at leading twist,

$$\Delta^{[\gamma^-]} = D_1(z_h, \xi, \vec{k}_T^2, \vec{R}_T^2, \vec{k}_T \cdot \vec{R}_T) \quad (8a)$$

$$\Delta^{[\gamma^- \gamma_5]} = \frac{\epsilon_T^{ij} R_{Ti} k_{Tj}}{M_1 M_2} G_1^\perp(z_h, \xi, \vec{k}_T^2, \vec{R}_T^2, \vec{k}_T \cdot \vec{R}_T) \quad (8b)$$

$$\begin{aligned} \Delta^{[i\sigma^{i-} \gamma_5]} &= \frac{\epsilon_T^{ij} R_{Tj}}{M_1 + M_2} H_1^\times(z_h, \xi, \vec{k}_T^2, \vec{R}_T^2, \vec{k}_T \cdot \vec{R}_T) \\ &+ \frac{\epsilon_T^{ij} k_{Tj}}{M_1 + M_2} H_1^\perp(z_h, \xi, \vec{k}_T^2, \vec{R}_T^2, \vec{k}_T \cdot \vec{R}_T). \end{aligned} \quad (8c)$$

The leading-twist projections give a nice probabilistic interpretation of FF related to the matrix  $\Gamma$  used. Hence,  $D_1$  is the probability for a unpolarized quark to fragment into the unpolarized hadron pair,  $G_1^\perp$  is the probability difference for a longitudinally polarized quark with opposite chiralities to

fragment into the pair, both  $H_1^\perp$  and  $H_1^\times$  give the same probability difference but for a transversely polarized fragmenting quark. A different interpretation for  $H_1^\perp$  and  $H_1^\times$  comes only from the possible origin for a non-vanishing probability difference, which is induced by the direction of  $k_T$  and  $R_T$ , respectively.  $G_1^\perp, H_1^\perp, H_1^\times$  are all naive  $T$ -odd and  $H_1^\perp, H_1^\times$  are further chiral odd.  $H_1^\perp$  represents a sort of generalization of the Collins effect, while  $H_1^\times$  originates from a genuine new effect, because it relates the transverse polarization of the fragmenting quark to the orbital angular motion of the transverse component of the pair relative momentum  $\vec{R}_T$  via the new angle  $\phi$ , defined by

$$\begin{aligned} \sin \phi &= \frac{\vec{S}'_T \cdot \vec{P}_2 \times \vec{P}_1}{|\vec{S}'_T| |\vec{P}_2 \times \vec{P}_1|} = \frac{\vec{S}'_T \cdot \vec{P}_h \times \vec{R}}{|\vec{S}'_T| |\vec{P}_h \times \vec{R}|} \\ &\equiv \frac{\vec{S}'_T \cdot \vec{P}_h \times \vec{R}_T}{|\vec{S}'_T| |\vec{P}_h \times \vec{R}_T|} \\ &= \cos \left( \phi_{S'_T} - \frac{\pi}{2} - \phi_{R_T} \right) = \sin(\phi_{S'_T} + \phi_{R_T}), \end{aligned} \quad (9)$$

where we have used the condition  $\vec{P}_{hT} = 0$  and  $\phi_{S'_T}$  ( $\phi_{S'_T}$ ),  $\phi_{R_T}$  are the azimuthal angles of the initial (final) quark transverse polarization and of  $\vec{R}_T$  with respect to the scattering plane, respectively (see also Fig. 2).

## B. Isolating transversity from the SSA

Usually, the analysis of experimental observables is better accomplished in the frame where the target momentum  $P$  and the momentum transfer  $q$  are collinear and with no transverse components. Using a different notation, we have  $\vec{P}_\perp = \vec{q}_\perp = 0$  and  $\vec{P}_{h\perp} \neq 0$ . An appropriate transverse Lorentz boost transforms this frame to the previous one where  $\vec{P}_T = \vec{P}_{hT} = 0$  and  $\vec{q}_T = -\vec{P}_{h\perp}/z$  [12]. However, the difference between the components of vectors in each frame is suppressed like  $\mathcal{O}(1/Q)$ . Since we are here considering expressions for the observables at leading twist only, this difference can be safely neglected.

By using Eq. (5), the complete cross section at leading twist for the two-hadron inclusive DIS of an unpolarized beam on a transversely polarized target, where two unpolarized hadrons are detected in the same quark current jet, is given by

$$\begin{aligned} \frac{d\sigma}{d\Omega dx dz d\xi d^2\vec{P}_{h\perp} dM_h^2 d\phi_{R_\perp}} \\ = \frac{\xi(1-\xi)}{2} \frac{d\sigma}{d\Omega dx dz d\xi d^2\vec{P}_{h\perp} d^2\vec{R}_\perp} = \frac{d\sigma_{OO}}{d\Omega dx dz d\xi d^2\vec{P}_{h\perp} dM_h^2 d\phi_{R_\perp}} + |\vec{S}_\perp| \frac{d\sigma_{OT}}{d\Omega dx dz d\xi d^2\vec{P}_{h\perp} dM_h^2 d\phi_{R_\perp}} \end{aligned}$$

$$\begin{aligned}
&= \frac{\alpha_{em} s x}{(2\pi)^3 2Q^4} \left\{ A(y) \mathcal{F}[f_1 D_1] + |\vec{R}_\perp| B(y) \sin(\phi_h + \phi_{R_\perp}) \mathcal{F} \left[ \hat{g} \cdot \vec{p}_T \frac{h_1^\perp H_1^\times}{M(M_1 + M_2)} \right] - |\vec{R}_\perp| B(y) \cos(\phi_h + \phi_{R_\perp}) \right. \\
&\quad \times \mathcal{F} \left[ \hat{h} \cdot \vec{p}_T \frac{h_1^\perp H_1^\times}{M(M_1 + M_2)} \right] - B(y) \cos(2\phi_h) \mathcal{F} \left[ (2\hat{h} \cdot \vec{p}_T \hat{h} \cdot \vec{k}_T - \vec{p}_T \cdot \vec{k}_T) \frac{h_1^\perp H_1^\perp}{M(M_1 + M_2)} \right] \\
&\quad \left. - B(y) \sin(2\phi_h) \mathcal{F} \left[ (\hat{h} \cdot \vec{p}_T \hat{g} \cdot \vec{k}_T + \hat{h} \cdot \vec{k}_T \hat{g} \cdot \vec{p}_T) \frac{h_1^\perp H_1^\perp}{M(M_1 + M_2)} \right] \right\} \\
&\quad + \frac{\alpha_{em} s x}{(2\pi)^3 2Q^4} |\vec{S}_\perp| \left\{ A(y) \sin(\phi_h - \phi_{S_\perp}) \mathcal{F} \left[ \hat{h} \cdot \vec{p}_T \frac{f_{1T}^\perp D_1}{M} \right] + A(y) \cos(\phi_h - \phi_{S_\perp}) \mathcal{F} \left[ \hat{g} \cdot \vec{p}_T \frac{f_{1T}^\perp D_1}{M} \right] \right. \\
&\quad + B(y) \sin(\phi_h + \phi_{S_\perp}) \mathcal{F} \left[ \hat{h} \cdot \vec{k}_T \frac{h_1 H_1^\perp}{M_1 + M_2} \right] + B(y) \cos(\phi_h + \phi_{S_\perp}) \mathcal{F} \left[ \hat{g} \cdot \vec{k}_T \frac{h_1 H_1^\perp}{M_1 + M_2} \right] \\
&\quad + |\vec{R}_\perp| B(y) \sin(\phi_{R_\perp} + \phi_{S_\perp}) \mathcal{F} \left[ \frac{h_1 H_1^\times}{M_1 + M_2} \right] - |\vec{R}_\perp| A(y) \cos(\phi_h - \phi_{S_\perp}) \sin(\phi_h - \phi_{R_\perp}) \\
&\quad \times \mathcal{F} \left[ \hat{h} \cdot \vec{k}_T \hat{h} \cdot \vec{p}_T \frac{g_{1T} G_1^\perp}{M M_1 M_2} \right] + |\vec{R}_\perp| A(y) \sin(\phi_h - \phi_{S_\perp}) \sin(\phi_h - \phi_{R_\perp}) \mathcal{F} \left[ \hat{h} \cdot \vec{k}_T \hat{g} \cdot \vec{p}_T \frac{g_{1T} G_1^\perp}{M M_1 M_2} \right] \\
&\quad - |\vec{R}_\perp| A(y) \cos(\phi_h - \phi_{S_\perp}) \cos(\phi_h - \phi_{R_\perp}) \mathcal{F} \left[ \hat{g} \cdot \vec{k}_T \hat{h} \cdot \vec{p}_T \frac{g_{1T} G_1^\perp}{M M_1 M_2} \right] + |\vec{R}_\perp| A(y) \sin(\phi_h - \phi_{S_\perp}) \cos(\phi_h - \phi_{R_\perp}) \\
&\quad \times \mathcal{F} \left[ \hat{g} \cdot \vec{k}_T \hat{g} \cdot \vec{p}_T \frac{g_{1T} G_1^\perp}{M M_1 M_2} \right] + B(y) \cos(3\phi_h - \phi_{S_\perp}) \mathcal{F} \left[ \hat{h} \cdot \vec{k}_T \hat{h} \cdot \vec{p}_T \hat{g} \cdot \vec{p}_T \frac{h_1^\perp H_1^\perp}{M^2(M_1 + M_2)} \right] + B(y) \sin(2\phi_h) \cos(\phi_h - \phi_{S_\perp}) \\
&\quad \times \mathcal{F} \left[ \hat{h} \cdot \vec{k}_T (\hat{h} \cdot \vec{p}_T)^2 \frac{h_{1T}^\perp H_1^\perp}{M^2(M_1 + M_2)} \right] - B(y) \cos(2\phi_h) \sin(\phi_h - \phi_{S_\perp}) \mathcal{F} \left[ \hat{h} \cdot \vec{k}_T (\hat{g} \cdot \vec{p}_T)^2 \frac{h_{1T}^\perp H_1^\perp}{M^2(M_1 + M_2)} \right] - B(y) \sin(3\phi_h - \phi_{S_\perp}) \\
&\quad \times \mathcal{F} \left[ \hat{g} \cdot \vec{k}_T \hat{h} \cdot \vec{p}_T \hat{g} \cdot \vec{p}_T \frac{h_{1T}^\perp H_1^\perp}{M^2(M_1 + M_2)} \right] + B(y) \cos(2\phi_h) \cos(\phi_h - \phi_{S_\perp}) \mathcal{F} \left[ \hat{g} \cdot \vec{k}_T (\hat{h} \cdot \vec{p}_T)^2 \frac{h_{1T}^\perp H_1^\perp}{M^2(M_1 + M_2)} \right] \\
&\quad + B(y) \sin(2\phi_h) \sin(\phi_h - \phi_{S_\perp}) \mathcal{F} \left[ \hat{g} \cdot \vec{k}_T (\hat{g} \cdot \vec{p}_T)^2 \frac{h_{1T}^\perp H_1^\perp}{M^2(M_1 + M_2)} \right] + |\vec{R}_\perp| B(y) \sin(2\phi_h + \phi_{R_\perp} - \phi_{S_\perp}) \\
&\quad \left. \times \mathcal{F} \left[ [(\hat{h} \cdot \vec{p}_T)^2 - (\hat{g} \cdot \vec{p}_T)^2 + 2\hat{h} \cdot \vec{p}_T \hat{g} \cdot \vec{p}_T] \frac{h_{1T}^\perp H_1^\times}{2M^2(M_1 + M_2)} \right] \right\}, \tag{10}
\end{aligned}$$

where  $\alpha_{em}$  is the fine structure constant,  $s = Q^2/xy = -q^2/xy$  is the total energy in the center-of-mass system and

$$\begin{aligned}
A(y) &= \left( 1 - y + \frac{1}{2} y^2 \right), & B(y) &= (1 - y), \\
C(y) &= y(2 - y), \tag{11}
\end{aligned}$$

where the lepton with 4-momentum  $l$  is detected in the solid angle  $d\Omega$  and  $y = (P \cdot q)/(P \cdot l) \approx q^-/l^-$ . The convolution of distribution and fragmentation functions is defined as

$$\begin{aligned}
\mathcal{F}[w(\vec{p}_T, \vec{k}_T) f D] &\equiv \sum_a e_a^2 \int d^2\vec{p}_T d^2\vec{k}_T \\
&\quad \times \delta^2 \left( \vec{k}_T - \vec{p}_T + \frac{\vec{P}_{h\perp}}{z} \right) w(\vec{p}_T, \vec{k}_T) \\
&\quad \times f^a(x, \vec{p}_T^2) D^a(z_h, \xi, \vec{k}_T^2, \vec{R}_T^2, \vec{k}_T \cdot \vec{R}_T), \tag{12}
\end{aligned}$$

where  $w(\vec{p}_T, \vec{k}_T)$  is a weight function and the sum runs over all quark (and anti-quark) flavors, with  $e_a$  the electric charges of the quarks. The unit vectors appearing in the

weight function  $w$  are defined as  $\hat{h} = \vec{P}_{h\perp} / |\vec{P}_{h\perp}|$  and  $\hat{g}^i = \epsilon^{ij} \hat{h}^j$  (with  $\epsilon^{ij} \equiv \epsilon^{-+ij}$ ), respectively, and they represent the two independent directions in the  $\perp$  plane perpendicular to  $\hat{z} \parallel \vec{q} / |\vec{q}|$ . All azimuthal angles  $\phi_{S\perp}, \phi_{R\perp}$  and  $\phi_h$  (relative to  $\vec{P}_{h\perp}$ ) lie in the  $\perp$  plane and are measured with respect to the scattering plane (see Fig. 3). Equation (10) corresponds to the sum of Eqs. (B1) and (B4) in Ref. [12], where, however, the expressions are simpler because they rely on the assumption of a symmetrical cylindrical distribution of hadron pairs around the jet axis in order to have fragmentation functions depending on even powers of  $\vec{k}_T$  only [this assumption would make all terms including the  $\hat{g}$  versor disappear from Eq. (10); see also Ref. [20] for a comparison].

During experiments the scattering plane changes (different scales  $Q$  imply different positions of the scattered beam). Therefore, it is better to define the laboratory frame as the plane formed by the beam and the direction of the target polarization. All azimuthal angles are conveniently reexpressed with respect to the laboratory frame as

$$\begin{aligned}\phi_{R\perp} &= \phi_{R\perp}^L - \phi^L \\ \phi_{S\perp} &= -\phi^L \\ \phi_h &= \phi_h^L - \phi^L,\end{aligned}\tag{13}$$

where the superscript “ $L$ ” indicates the new reference frame. The oriented angle between the scattering plane and the laboratory frame is  $\phi^L$  (see Fig. 3). At leading order, the azimuthal angle of Eq. (9) becomes  $\phi = \phi_{R\perp}^L - 2\phi^L$  in the new frame.

The new expression for the cross section is obtained by simply replacing Eq. (13) inside the angular dependence of Eq. (10). After replacement and apart from phase space coefficients, each term of the cross section will look like

$$\begin{aligned}d\sigma^{tw} &\propto t(\phi_{R\perp}^L, \phi^L, \phi_h^L) \mathcal{F}[w \text{ DF FF}] \\ &= t(\phi_{R\perp}^L, \phi^L, \phi_h^L) I(z, \xi, \vec{R}_T^2),\end{aligned}\tag{14}$$

where  $t$  is a trigonometric function,  $w$  is the specific weight function for each combination of distribution and fragmentation functions (DF and FF, respectively), and  $I$  is the result of the convolution integral. It is easy to verify that folding the cross section by

$$\begin{aligned}\frac{1}{2\pi} \int_0^{2\pi} d\phi^L d\phi_{R\perp}^L \sin(\phi_{R\perp}^L - 2\phi^L) \\ \times \frac{d\sigma}{d\Omega dx dz d\xi d^2\vec{P}_{h\perp} dM_h^2 d\phi_{R\perp}}\end{aligned}\tag{15}$$

makes only those  $d\sigma^{tw}$  terms survive where  $H_1^*$  shows up in the convolution, i.e. for the following combinations:

$$t = \cos(\phi_h^L + \phi_{R\perp}^L - 2\phi^L), \quad w = \hat{h} \cdot \vec{p}_T,\tag{16a}$$

$$t = \sin(\phi_h^L + \phi_{R\perp}^L - 2\phi^L), \quad w = \hat{g} \cdot \vec{p}_T,\tag{16b}$$

$$t = \sin(\phi_{R\perp}^L - 2\phi^L), \quad w = 1,\tag{16c}$$

$$t = \sin(2\phi_h^L + \phi_{R\perp}^L - 2\phi^L),$$

$$w = (\hat{h} \cdot \vec{p}_T)^2 - (\hat{g} \cdot \vec{p}_T)^2 + 2\hat{h} \cdot \vec{p}_T \hat{g} \cdot \vec{p}_T.\tag{16d}$$

Similarly, it is straightforward to prove that integrating these surviving terms upon  $d^2\vec{P}_{h\perp}$ , and performing the integrals in the convolution  $\mathcal{F}[w \text{ DF FF}]$ , makes only the combination (16c) survive, presenting the transversity in a factorized form. In fact, by integrating also upon  $d\xi$ , we finally have

$$\begin{aligned}\frac{\langle d\sigma_{OT} \rangle}{dy dx dz dM_h^2} &\equiv \frac{1}{2\pi} \int_0^{2\pi} d\phi^L d\phi_{R\perp}^L \int d^2\vec{P}_{h\perp} \int d\xi \sin(\phi_{R\perp}^L - 2\phi^L) \frac{d\sigma}{d\Omega dx dz d\xi dM_h^2 d\phi_{R\perp}^L d^2\vec{P}_{h\perp}} \\ &= \frac{\pi \alpha_{em}^2 s x}{(2\pi)^3 Q^4} \frac{B(y) |\vec{S}_\perp|}{2(M_1 + M_2)} \sum_a e_a^2 \int d^2\vec{p}_T h_1^a(x, \vec{p}_T^2) \int d\xi |\vec{R}_\perp| \int_0^{2\pi} d\phi_{R\perp}^L \int d^2\vec{k}_T H_{1(R)}^{*a}(z, \xi, M_h^2, \vec{k}_T^2, \vec{k}_T \cdot \vec{R}_T) \\ &\equiv \frac{\pi \alpha_{em}^2 s}{(2\pi)^3 Q^4} B(y) |\vec{S}_\perp| \sum_a e_a^2 x h_1^a(x) H_{1(R)}^{*a}(z, M_h^2),\end{aligned}\tag{17}$$

where, for the sake of simplicity, the same notations are kept for DF and FF before and after integration, distinguishing them by the explicit arguments only; the subscript  $(R)$  reminds of the additional dimensionless weighting factor  $|\vec{R}_\perp|/2(M_1 + M_2)$ . Analogously,

$$\begin{aligned}
\frac{\langle d\sigma_{OO} \rangle}{dy dx dz dM_h^2} &\equiv \frac{1}{2\pi} \int_0^{2\pi} d\phi^L d\phi_{R\perp}^L \int d^2\vec{P}_{h\perp} \int d\xi \frac{d\sigma}{d\Omega dx dz d\xi dM_h^2 d\phi_{R\perp}^L d^2\vec{P}_{h\perp}} \\
&= \frac{\pi\alpha_{em}^2 s x}{(2\pi)^3 Q^4} A(y) \sum_a e_a^2 \int d^2\vec{p}_T f_1^a(x, \vec{p}_T^2) \int d\xi \int_0^{2\pi} d\phi_{R\perp}^L \int d^2\vec{k}_T D_1^a(z, \xi, M_h^2, \vec{k}_T^2, \vec{k}_T \cdot \vec{R}_T) \\
&\equiv \frac{\pi\alpha_{em}^2 s}{(2\pi)^3 Q^4} A(y) \sum_a e_a^2 x f_1^a(x) D_1^a(z, M_h^2), \tag{18}
\end{aligned}$$

from which we can build the single spin asymmetry

$$\begin{aligned}
A^{\sin\phi}(y, x, z, M_h^2) &\equiv \frac{\langle d\sigma_{OT} \rangle}{dy dx dz dM_h^2} \left[ \frac{\langle d\sigma_{OO} \rangle}{dy dx dz dM_h^2} \right]^{-1} \\
&= \frac{B(y)}{A(y)} \frac{|\vec{S}_\perp| \sum_a e_a^2 x h_1^a(x) H_{1(R)}^{\chi_a}(z, M_h^2)}{\sum_a e_a^2 x f_1^a(x) D_1^a(z, M_h^2)}. \tag{19}
\end{aligned}$$

### III. SPECTATOR MODEL FOR $\pi^+ \pi^-$ FRAGMENTATION

In the field theoretical description of hard processes, the FF represent the soft processes that connect the hard quark to the detected hadrons via fragmentation, i.e. they are hadronic matrix elements of nonlocal operators built from quark (and gluon) fields [21]. For a quark fragmenting into two hadrons inside the same current jet, the appropriate quark-quark correlator (in the light-cone gauge) reads [10,9]

$$\begin{aligned}
\Delta_{ij}(k, P_1, P_2) &= \sum_X \int \frac{d^4\zeta}{(2\pi)^4} e^{ik \cdot \zeta} \langle 0 | \psi_i(\zeta) | P_1, P_2, X \rangle \\
&\quad \times \langle X, P_2, P_1 | \bar{\psi}_j(0) | 0 \rangle, \tag{20}
\end{aligned}$$

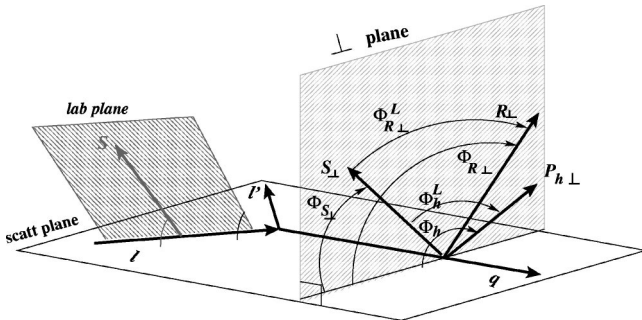


FIG. 3. The definition of azimuthal angles, in the frame where  $q_\perp = 0$ , with respect to the scattering plane and the laboratory plane, whose relative oriented angle is  $\phi^L = -\phi_{S_\perp}$ .

where the sum runs over all the possible intermediate states containing the hadron pair.

The basic idea of the spectator model is to make a specific ansatz for this spectral decomposition by replacing the sum with an effective spectator state with a definite mass and quantum numbers [16,17,19]. By specializing the model to the case of  $\pi^+ \pi^-$  fragmentation with  $P_1 = P_{\pi^+}$  and  $P_2 = P_{\pi^-}$ , the spectator has the quantum numbers of an on-shell valence quark with a constituent mass  $m_q = 340$  MeV. Consequently, the quark-quark correlator (20) simplifies to

$$\begin{aligned}
\Delta_{ij}(k, P_{\pi^+}, P_{\pi^-}) &\approx \frac{\theta((k - P_h)^+)}{(2\pi)^3} \delta((k - P_h)^2 - m_q^2) \\
&\quad \times \langle 0 | \psi_i(0) | P_{\pi^+}, P_{\pi^-}, q \rangle \\
&\quad \times \langle q, P_{\pi^-}, P_{\pi^+} | \bar{\psi}_j(0) | 0 \rangle \\
&\equiv \tilde{\Delta}_{ij}(k, P_{\pi^+}, P_{\pi^-}) \\
&\quad \times \delta(\tau_h - \sigma_h + M_h^2 - m_q^2), \tag{21}
\end{aligned}$$

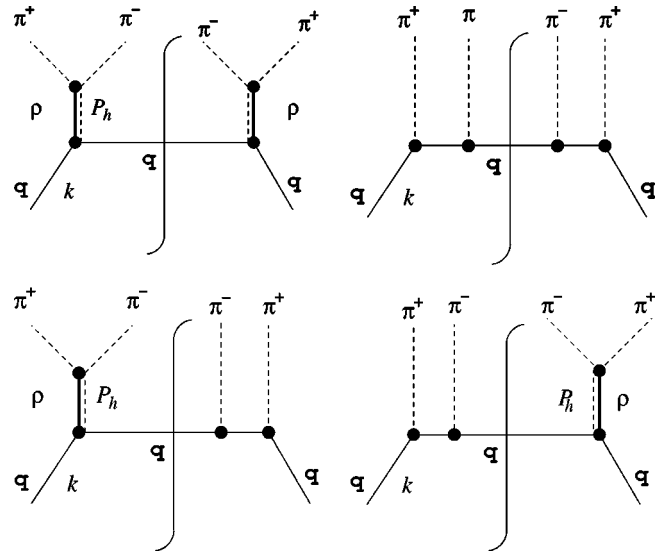


FIG. 4. The diagrams considered for the quark fragmentation into  $\pi^+ \pi^-$  at leading twist and leading order in  $\alpha_s$  in the context of the spectator model.

where  $\tau_h = k^2$  and  $\sigma_h = 2k \cdot P_h$ . When inserting Eq. (21) into Eq. (7), the projections drastically simplify to

$$\Delta^{[\Gamma]}(z_h, \xi, \vec{k}_T^2, \vec{R}_T^2, \vec{k}_T \cdot \vec{R}_T) = \frac{\text{Tr}[\Gamma \tilde{\Delta}]}{8(1-z)P_h^-} \Bigg|_{\tau_h = \tau_h(z, \vec{k}_T^2)}, \quad (22)$$

with

$$\tau_h(z, \vec{k}_T^2) = \frac{z}{1-z} \vec{k}_T^2 + \frac{m_q^2}{1-z} + \frac{M_h^2}{z}. \quad (23)$$

We will consider the  $\pi^+ \pi^-$  system with an invariant mass  $M_h$  close to the  $\rho$  resonance, specifically  $m_\rho - \Gamma_\rho/2 \leq M_h \leq m_\rho + \Gamma_\rho/2$ , where  $\Gamma_\rho$  is the width of the  $\rho$  resonance. Hence, the most appropriate and simplest diagrams that can replace the quark decay of Fig. 1 at leading twist, and lead-

ing order in  $\alpha_s$ , are represented in Fig. 4: the  $\pi^+ \pi^-$  can be produced from the  $\rho$  decay or directly via a quark exchange in the  $t$  channel (the background diagram); the quantum interference of the two processes generates the *naive*  $T$ -odd FF described in Sec. II A. In Appendix A, a suitable selection of ‘‘Feynman rules’’ for the vertices and propagators of the diagrams in Fig. 4 is defined that allows for the analytic calculation of the matrix elements defining  $\tilde{\Delta}$  in Eq. (21) and, consequently, of the projections  $\Delta^{[\Gamma]}$  in Eq. (22) defining the FF.

The *naive*  $T$ -odd  $G_1^\perp, H_1^\perp, H_1^*$  receive contributions from the interference diagrams only. In particular, they result proportional to the imaginary part of the  $\rho$  propagator ( $\sim m_\rho \Gamma_\rho$ ), while the real part ( $\sim M_h^2 - m_\rho^2$ ) contributes to  $D_1$ . Therefore, contrary to the findings of Ref. [11], a complex amplitude with a resonant behavior is needed here to produce nonvanishing interference FF. For a  $u$  quark fragmenting into  $\pi^+ \pi^-$ , we have at leading twist

$$\begin{aligned} D_1^{u \rightarrow \pi^+ \pi^-}(z, \xi, M_h^2, k_T^2, \vec{k}_T \cdot \vec{R}_T) &= \frac{N_{q\rho}^2 f_\rho^2 \pi^2 z^2 (1-z)^2}{4(2\pi)^3 [(M_h^2 - m_\rho^2)^2 + m_\rho^2 \Gamma_\rho^2] a^2 |a+b|^3} \left\{ \frac{c}{4} [c - za(2\xi - 1)] + z^2(1-z) \left( \frac{M_h^2}{4} - m_\pi^2 \right) \right. \\ &\times [a - (1-z)M_h^2] \left. \right\} + \frac{N_{q\pi}^4 z^7 (1-z)^7}{8(2\pi)^3 a^2 d^2 |d+\bar{b}|^3 |a+\bar{b}|^3} \left\{ -az[z\xi(1-z) + (1-\xi)d] - z(1-z) \right. \\ &\times m_\pi^2 \frac{a-c-z(1-z)M_h^2}{2} + d \frac{a-c+z(1-z)M_h^2}{2} \left. \right\} \\ &+ \frac{\sqrt{2}(M_h^2 - m_\rho^2) z^{9/2} (1-z)^{9/2} N_{q\pi}^2 N_{q\rho} f_\rho \pi \pi}{8(2\pi)^3 [(M_h^2 - m_\rho^2)^2 + m_\rho^2 \Gamma_\rho^2] a^2 d |a+b|^{3/2} |a+\bar{b}|^{3/2} |d+\bar{b}|^{3/2}} \left\{ az(1-z) \left( 2m_\pi^2 - \frac{M_h^2}{2} \right) \right. \\ &+ \frac{a(1-2z\xi) + c + z(1-z)M_h^2}{4} [d + z(1-z)(M_h^2 - 5m_\pi^2)] \\ &\left. + \frac{a[2z(1-\xi) - 1] + c - z(1-z)M_h^2}{4} [3d - a + z(1-z)m_\pi^2] \right\} \end{aligned} \quad (24)$$

$$H_1^{*u \rightarrow \pi^+ \pi^-}(z, \xi, M_h^2, k_T^2, \vec{k}_T \cdot \vec{R}_T) = - \frac{m_\rho \Gamma_\rho m_\pi m_q z^{13/2} (1-z)^{11/2} N_{q\pi}^2 N_{q\rho} f_\rho \pi \pi}{2\sqrt{2}(2\pi)^3 [(M_h^2 - m_\rho^2)^2 + m_\rho^2 \Gamma_\rho^2] a d |a+b|^{3/2} |a+\bar{b}|^{3/2} |d+z(1-z)(m_q^2 - \Lambda_\pi^2)|^{3/2}} \quad (25)$$

$$H_1^{\perp u \rightarrow \pi^+ \pi^-}(z, \xi, M_h^2, k_T^2, \vec{k}_T \cdot \vec{R}_T) = 0 \quad (26)$$

$$G_1^{\perp u \rightarrow \pi^+ \pi^-}(z, \xi, M_h^2, k_T^2, \vec{k}_T \cdot \vec{R}_T) = - \frac{m_\pi}{2m_q} H_1^{*u \rightarrow \pi^+ \pi^-}(z, \xi, M_h^2, k_T^2, \vec{k}_T \cdot \vec{R}_T), \quad (27)$$

where

$$a = z^2(k_T^2 + m_q^2) + (1-z)M_h^2,$$

$$b = z(1-z)(m_q^2 - \Lambda_\pi^2),$$

$$\bar{b} = z(1-z)(m_q^2 - \Lambda_\pi^2)$$

$$c = (2\xi - 1)[z^2(k_T^2 + m_q^2) - (1-z)^2 M_h^2]$$

$$-4z(1-z)\vec{k}_T \cdot \vec{R}_T \quad (28)$$



$$d = z^2(1-\xi)(k_T^2 + m_q^2) + \xi(1-z)^2 M_h^2 \\ + z(1-z)(m_\pi^2 + 2\vec{k}_T \cdot \vec{R}_T).$$

The simplifications induced by the spectator model reduce the number of independent FF, Eq. (27), and make  $H_1^\perp$  vanish, i.e. the analogue of the Collins effect in this context turns out to be a higher-order effect. The structure induced by the model is simply not rich enough to produce a non-vanishing  $H_1^\perp$ . Moreover, the FF do not depend on the flavor of the fragmenting valence quark, provided that the charges of the final detected pions are selected according to the diagrams of Fig. 4. Hence, the FF are the same for  $u \rightarrow \pi^+ \pi^-$  and for  $d \rightarrow \pi^- \pi^+$ , where the final state differs only by the interchange of the two pions, i.e. by leaving everything unaltered but  $\vec{R}_T \rightarrow -\vec{R}_T$  and  $\xi \rightarrow (1-\xi)$ :

$$D_1^{u \rightarrow \pi^+ \pi^-}(z, \xi, M_h^2, k_T^2, \vec{k}_T \cdot \vec{R}_T) \\ = D_1^{d \rightarrow \pi^- \pi^+}(z, \xi, M_h^2, k_T^2, \vec{k}_T \cdot \vec{R}_T) \\ = D_1^{d \rightarrow \pi^+ \pi^-}(z, (1-\xi), M_h^2, k_T^2, \vec{k}_T \cdot (-\vec{R}_T)) \\ H_1^{\times u \rightarrow \pi^+ \pi^-}(z, \xi, M_h^2, k_T^2, \vec{k}_T \cdot \vec{R}_T) \\ = H_1^{\times d \rightarrow \pi^- \pi^+}(z, \xi, M_h^2, k_T^2, \vec{k}_T \cdot \vec{R}_T) \\ = H_1^{\times d \rightarrow \pi^+ \pi^-}(z, (1-\xi), M_h^2, k_T^2, \vec{k}_T \cdot (-\vec{R}_T)). \quad (29)$$

When integrating the FF over  $d^2\vec{k}_T$  and  $d\xi$ , the dependence on the direction of  $\vec{R}_T$  is lost:

$$D_1^{u \rightarrow \pi^+ \pi^-}(z, M_h^2) \\ \equiv \int_0^1 d\xi \int d^2\vec{k}_T D_1^{u \rightarrow \pi^+ \pi^-}(z, \xi, M_h^2, k_T^2, \vec{k}_T \cdot \vec{R}_T)$$

$$= \int_0^1 d\xi \int d^2\vec{k}_T \\ \times D_1^{d \rightarrow \pi^+ \pi^-}(z, (1-\xi), M_h^2, k_T^2, \vec{k}_T \cdot (-\vec{R}_T)) \\ = \int_0^1 d\xi \int d^2\vec{k}_T D_1^{d \rightarrow \pi^+ \pi^-}(z, \xi, M_h^2, k_T^2, \vec{k}_T \cdot (-\vec{R}_T)) \\ \equiv D_1^{d \rightarrow \pi^+ \pi^-}(z, M_h^2), \quad (30)$$

and similarly for  $H_1^{\times}$ . Therefore, we can conclude that the integrated FF do not depend in general on the flavor of the fragmenting quark.

Consequently, the SSA of Eq. (19) simplifies to

$$A^{\sin \phi}(y, x, z, M_h^2) \\ = \frac{B(y)}{A(y)} |\vec{S}_\perp| \\ \times \frac{\left[ \frac{8}{9} x h_1^u(x) + \frac{1}{9} x h_1^d(x) \right] H_{1(R)}^{\times u}(z, M_h^2)}{\left[ \frac{8}{9} x f_1^u(x) + \frac{1}{9} x f_1^d(x) \right] D_1^u(z, M_h^2)}. \quad (31)$$

In the following, we will discuss the SSA without the inessential  $|\vec{S}_\perp| B(y)/A(y)$  factor and after integrating away the  $z$  dependence and, in turn, the  $x$  or  $M_h$  dependence according to

$$A_x^{\sin \phi}(x) \equiv \frac{\left[ \frac{8}{9} x h_1^u(x) + \frac{1}{9} x h_1^d(x) \right] \int dz dM_h^2 H_{1(R)}^{\times u}(z, M_h^2)}{\left[ \frac{8}{9} x f_1^u(x) + \frac{1}{9} x f_1^d(x) \right] \int dz dM_h^2 D_1^u(z, M_h^2)} \quad (32)$$

$$A_{M_h}^{\sin \phi}(M_h) \equiv \frac{\int dx \left[ \frac{8}{9} x h_1^u(x) + \frac{1}{9} x h_1^d(x) \right] \int dz H_{1(R)}^{\times u}(z, M_h^2)}{\int dx \left[ \frac{8}{9} x f_1^u(x) + \frac{1}{9} x f_1^d(x) \right] \int dz D_1^u(z, M_h^2)}. \quad (33)$$

#### IV. NUMERICAL RESULTS

In the remainder of the paper, we present numerical results in the context of the spectator model for both the process-independent FF and the SSA of Eqs. (32) and (33)

for semi-inclusive lepton-nucleon DIS. Considering different possible scenarios for  $h_1$ , we argue about an actual measurability of these SSA and the implications for the extraction of the transversity.

The input parameters of the calculation can basically be

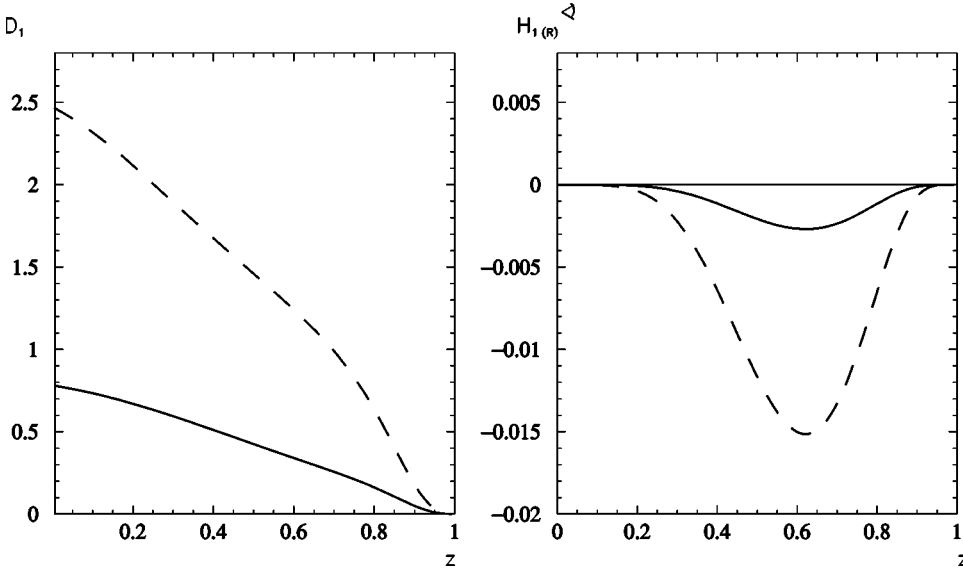


FIG. 5. The dimensionless integrated FF  $D_1(z)$  (left) and  $H_{1(R)}^{\chi_u}(z)$  (right), see text. Solid line for  $N_{q\rho}=0.9 \text{ GeV}^3$ , and the integral (B2) amounting to 0.14; dashed line for  $N_{q\rho}=1.6 \text{ GeV}^3$ , and the integral equals 0.48 (see the Appendixes).

grouped in three classes: values of masses and coupling constants taken from phenomenology, as  $m_\pi=0.139 \text{ GeV}$ ,  $m_\rho=0.785 \text{ GeV}$ , with  $f_{\rho\pi\pi}$  and  $\Gamma_\rho$  as described in Appendixes B and A, respectively; values consistent with other works on the spectator model and the constituent quark model, as  $\Lambda_\pi=0.4 \text{ GeV}$ ,  $\Lambda_\rho=0.5 \text{ GeV}$  and  $m_q=0.34 \text{ GeV}$  [17,19]; parameters, such as the  $q\pi q$  and  $q\rho q$  coupling strengths  $N_{q\pi}$  and  $N_{q\rho}$ , respectively, without constraints that are firmly established, or at least usually adopted, in the literature.

As described in Appendix B, the last ones are constrained using the integral (B2) and the proportionality (B4) derived from the Goldberger-Treiman relation. All results will be plotted according to two extreme scenarios, where the integral (B2) amounts to 0.14 ( $N_{q\rho}=0.9 \text{ GeV}^3$ , corresponding to solid lines in the figures) and 0.48 ( $N_{q\rho}=1.6 \text{ GeV}^3$ , corresponding to dashed lines in the figures). Because of the high degree of arbitrariness due to the lack of any data, the results should be interpreted as the indication not only of the sensitivity of the considered observables to the input parameters, but also of the degree of uncertainty that can be reached within the spectator model. In the same spirit, when dealing with the SSA of Eqs. (32), (33),  $f_1$  and  $h_1$  are calculated consistently within the spectator model [17] or, alternatively,  $f_1$  and  $g_1$  are taken from consistent parametrizations and  $h_1$  is calculated again according to two extreme scenarios: the nonrelativistic prediction  $h_1=g_1$  or the saturation of the Soffer inequality,  $h_1=(f_1+g_1)/2$ . The parametrizations for  $f_1, g_1$ , are extracted at the same lowest possible scale ( $Q^2=0.8 \text{ GeV}^2$ ), consistently with the valence quark approximation assumed for the calculation of the FF.

In Fig. 5 the dimensionless integrated  $D_1^u(z)$  and  $H_{1(R)}^{\chi_u}(z)$  are shown, according to the definitions of Eqs. (17) and (18), i.e.

$$\begin{aligned}
 D_1^u(z) &= \int_{a_\rho^2}^{b_\rho^2} dM_h^2 D_1(z, M_h^2) \\
 &= \int_{a_\rho^2}^{b_\rho^2} dM_h^2 \int d\xi \int_0^{2\pi} d\phi_{R_\perp}^L \int d^2\vec{k}_T \\
 &\quad \times D_1^u(z, \xi, M_h^2, \vec{k}_T^2, \vec{k}_T \cdot \vec{R}_T)
 \end{aligned} \tag{34}$$

$$\begin{aligned}
 H_{1(R)}^{\chi_u}(z) &= \int_{a_\rho^2}^{b_\rho^2} dM_h^2 H_{1(R)}^{\chi_u}(z, M_h^2) \\
 &= \int_{a_\rho^2}^{b_\rho^2} dM_h^2 \int d\xi \frac{|\vec{R}_\perp|}{4m_\pi} \int_0^{2\pi} d\phi_{R_\perp}^L \int d^2\vec{k}_T \\
 &\quad \times H_{1(R)}^{\chi_u}(z, \xi, M_h^2, \vec{k}_T^2, \vec{k}_T \cdot \vec{R}_T),
 \end{aligned} \tag{35}$$

where  $a_\rho=m_\rho-\Gamma_\rho/2$  and  $b_\rho=m_\rho+\Gamma_\rho/2$ . Again, we recall that the solid line corresponds to a weaker  $q\rho q$  coupling than the dashed line. The choice of the form factors at the vertices also guarantees the regular behavior at the end points  $z=0,1$ . The strongest asymmetry in the fragmentation (recall that  $H_1^{\chi_u}$  is defined as the probability difference for the fragmentation to proceed from a quark with opposite transverse polarizations) is reasonably reached at  $z\sim 0.4$ . Once again, we stress that this result, particularly its persistent negative sign, does not depend on a specific hard process and can influence the corresponding azimuthal asymmetry.

In fact, the SSA (32) and (33) for two-pion inclusive lepton-nucleon DIS as shown in Figs. 6 and 7, respectively, turn out to be negative due to the sign of  $H_{1(R)}^{\chi_u}$ . The solid and dashed lines again refer to the weaker or stronger  $q\rho q$  couplings in the FF, respectively. For each parametrization, three different choices of DF are shown. The label SP refers to the DF calculated in the spectator model [17]. The label NR indicates that  $f_1$  and  $g_1$  are taken consistently from the

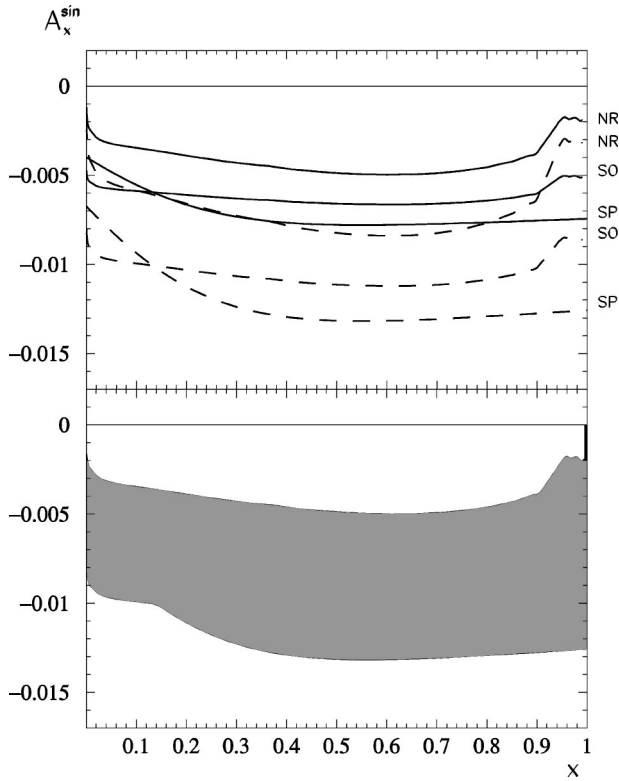


FIG. 6. The SSA of Eq. (32). In the upper plot, solid lines and dashed lines as in Fig. 5. Label SP stands for DF calculated in the spectator model [17]. Labels NR and SO indicate  $f_1$  from Ref. [22] and  $g_1$  from Ref. [23], but with  $h_1 = g_1$  and  $h_1 = (f_1 + g_1)/2$ , respectively. In the lower plot, the corresponding uncertainty band is shown (see text).

leading-order parametrizations of Refs. [22] and [23], respectively, with  $h_1 = g_1$ . The label SO indicates the same parametrizations but with the Soffer inequality saturated, i.e.  $h_1 = (f_1 + g_1)/2$ . In the lower plot of each figure the “uncertainty band” is shown as a guiding line. It is built by taking, for each  $z$  or  $M_h$ , the maximum and the minimum among the six curves displayed in the corresponding upper plot. The first obvious comment is that even the simple mechanism described in Fig. 4 produces a measurable asymmetry. For the HERMES experiment the size of the asymmetry may be at the lower edge of possible measurements, given the observed rather small average multiplicity which does not favor the detection of two pions in the final state. On the other hand, the planned transversely polarized target clearly will improve the situation of azimuthal spin-asymmetry measurements compared to the present one. COMPASS or possible future experiments at the ELFE, TESLA-N, or EIC facilities will have less problems because of higher counting rates. The second important result is that the sensitivity of the SSA to the parameters of the model calculation for the FF, and to the different parametrizations for the DF, is weak enough that the unambiguous message of a negative asymmetry emerges through all the range of both  $x$  and  $a_\rho = 0.69$  GeV  $\leq M_h \leq b_\rho = 0.84$  GeV. In particular, we do not find any change in sign for  $A_{M_h}^{\sin \phi}$ , contrary to what is predicted in Ref. [11].

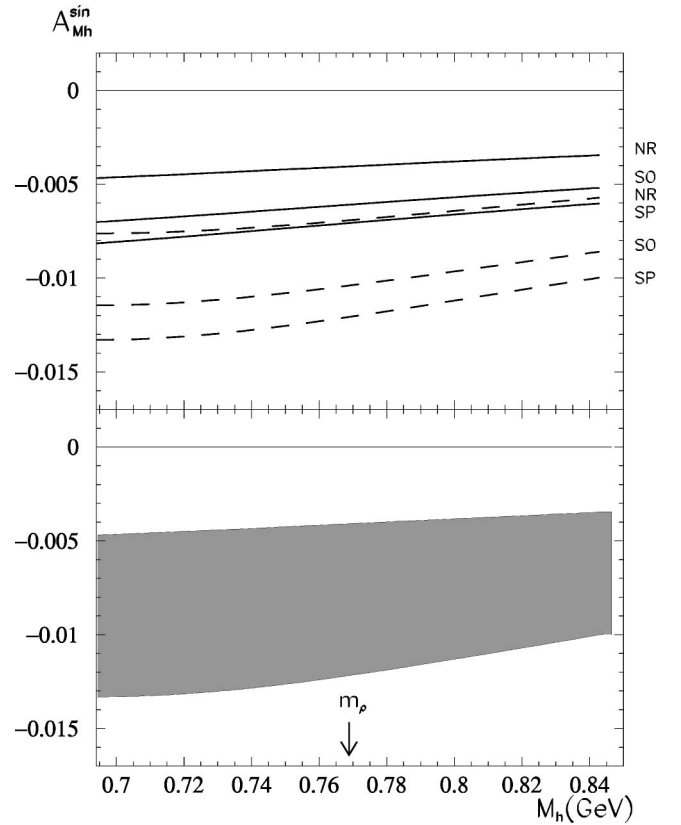


FIG. 7. The SSA of Eq. (33). In the upper plot, solid lines and dashed lines as in Fig. 5. Labels and meaning of lower plot as in Fig. 6.

## V. OUTLOOKS

In this paper we have discussed a way for addressing the transversity distribution  $h_1$  that we consider more advantageous, compared to other strategies discussed in the literature. At present, the SSA seem anyway preferable to the DSA. But the fragmentation of a transversely polarized quark into two unpolarized leading hadrons in the same current jet seems less complicated than the Collins effect, at least from the theoretical point of view. Collinear factorization implies an exact cancellation of the soft divergencies, avoiding any dilution of the asymmetry because of Sudakov form factors, and in principle it makes the QCD evolution simpler, though we have not addressed this subject in the present paper. The new effect, which allows for the extraction of  $h_1$  at leading twist through the new interference FF  $H_1^{\times}$ , relates the transverse polarization of the quark to the transverse component of the relative momentum of the hadron pair via a new azimuthal angle. This is the only key quantity to be determined experimentally, while the Collins effect requires the determination of the complete transverse momentum vector of the detected hadron.

We have shown also quantitative results for  $H_1^{\times}$  in the case of  $\pi^+ \pi^-$  detection, and the related SSA for the example of lepton-nucleon scattering. In fact, due the lack of any data and information about this class of FF, we believe that even the simple modelling of the interference between different channels, leading to the same final state, is a useful

resource to judge the reliability of this strategy for extracting the transversity distribution. Moreover, the scenario turns out to be simpler than the Collins effect, where a microscopic knowledge of the structure of the residual jet is required. We have adopted a spectator model approximation for  $\pi^+\pi^-$  with an invariant mass inside the  $\rho$  resonance width, limiting the process to leading-twist mechanisms. The interference between the decay of the  $\rho$  and the direct production of  $\pi^+\pi^-$  is enough to produce sizable and measurable asymmetries. Despite the theoretical uncertainty due to the arbitrariness in fixing the input parameters of the calculation of FF and in choosing the parametrizations for the DF, the unambiguous result emerges that, in the explored ranges in  $x$  and invariant mass  $M_h$ , the SSA are always negative and almost flat.

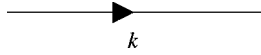
Anyway, it should be stressed again that the calculation has been performed at leading twist and in a valence-quark scenario. Therefore, higher-twist corrections and QCD evolution need to be explored before any realistic comparison with experiments could be attempted.

### ACKNOWLEDGMENTS

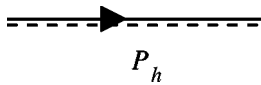
We acknowledge very fruitful discussions with Alessandro Bacchetta and Daniel Boer, in particular about the symmetry properties of the interference FF. This work has been supported by the TMR network HPRN-CT-2000-00130.

### APPENDIX A: PROPAGATORS

Here, we list the ‘‘Feynman rules’’ for the vertices and diagrams of Fig. 4 leading to Eqs. (24)–(27). The propagators involved in the diagrams of Fig. 4 are as follows. We have



quark with momentum  $\kappa$ :  $[i/(k-m_q)]_{ij}$ . The propagator occurs with  $\kappa^2 = \tau_h \equiv k^2$  or  $\kappa^2 = (k - P_{\pi^+})^2$ . In both cases, the off-shell condition  $k^2 \neq m_q^2$  is guaranteed by Eq. (23). We also have



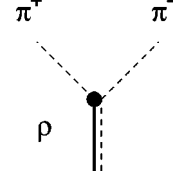
$\rho$  with momentum  $P_h$ :  $[i/(P_h^2 - m_\rho^2 + im_\rho \Gamma_\rho)] [-g^{\mu\nu} + (P_h^\mu P_h^\nu / P_h^2)]$ , where

$$\Gamma_\rho = (f_{\rho\pi\pi}^2/4\pi)(m_\rho/12)[1 - (4m_\pi^2/m_\rho^2)]^{3/2} \quad [24].$$

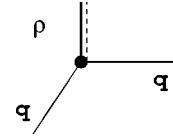
### APPENDIX B: VERTICES

In analogy with previous works on spectator models [17,19], we choose the vertex form factors to depend on one invariant only, generally denoted  $\kappa^2$ , that represents the virtuality of the external entering quark line. Therefore, we can have  $\kappa^2 = \tau_h \equiv k^2$  or  $\kappa^2 = (k - P_{\pi^+})^2$ . The power laws are such that the asymptotic behavior is in agreement with the

expectations based on dimensional counting rules. Finally, the normalization coefficients have dimensions such that  $\int d^2\vec{k}_T \int d^2\vec{R}_T D_1(z, \xi, \vec{k}_T^2, \vec{R}_T^2, \vec{k}_T \cdot \vec{R}_T)$  is a pure number to be interpreted as the probability for the hadron pair to carry a  $z$  fraction of the valence quark momentum and to share it in  $\xi$  and  $1 - \xi$  parts. We have



$\rho\pi\pi$  vertex:  $Y^{\rho\pi\pi,\mu} = f_{\rho\pi\pi} R^\mu$ , where  $f_{\rho\pi\pi}^2/4\pi = 2.84 \pm 0.50$  [25]. We also have



$q\rho q$  vertex:

$$\begin{aligned} Y_{ij}^{qq,\mu} &= [f_{qq\rho}(\kappa^2)/\sqrt{2}] [\gamma^\mu]_{ij} \\ &= (N_{q\rho}/\sqrt{2})(1/|\kappa^2 - \Lambda_\rho^2|^\alpha) [\gamma^\mu]_{ij} \end{aligned}$$

where  $\Lambda_\rho$  excludes large virtualities of the quark. The power  $\alpha$  is determined consistently with the quark counting rule that determines the asymptotic behavior of the FF at large  $z$  [25], i.e.

$$(1-z)^{2\alpha-1} = (1-z)^{-3+2r+2|\lambda|}, \quad (\text{B1})$$

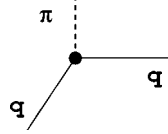
where  $r$  is the number of constituent quarks in the considered hadron, and  $\lambda$  is the difference between the quark and the hadron helicities. Thus, here we have  $\alpha = 3/2$ . The normalization  $N_{q\rho}$  is such that the sum rule

$$\int_0^1 dz z D_1(z) = \int_0^1 dz z \int_{a_\rho^2}^{b_\rho^2} dM_h^2 D_1(z, M_h^2) \leq 1 \quad (\text{B2})$$

is satisfied, with  $D_1(z, M_h^2)$  defined in Eq. (18). In fact, in the infinite momentum frame the integral in Eq. (B2) represents the total fraction  $z$  of the quark energy taken by all hadron pairs of the type under consideration. Since in this frame low-energy mass effects can be neglected, we estimate that charged pion pairs with an invariant mass inside the  $\rho$  resonance width represent  $\sim 50\%$  of the total pions detected in the calorimeter, which in turn can be considered  $\sim 80\%$  of all particles detected. Neglecting mass effects, we may assume that the fraction of quark energy taken by charged

pions, relative to the energy taken by other hadrons, follows their relative numbers. Therefore, we chose two values,  $N_{q\rho}=0.9 \text{ GeV}^3$  and  $1.6 \text{ GeV}^3$ , which correspond to rather extreme scenarios where the integral Eq. (B2) amounts to 0.14 and 0.48, respectively.

We also have



$q\pi q$  vertex:

$$Y_{ij}^{q\pi q} = [f_{q\pi q}(\kappa^2)/\sqrt{2}][\gamma_5]_{ij} = (N_{q\pi}/\sqrt{2})(1/|\kappa^2 - \Lambda_\pi^2|^\alpha) \times [\gamma_5]_{ij},$$

where  $\Lambda_\pi$  excludes large virtualities of the quark, as well. From quark counting rules, still  $\alpha=3/2$ . The normalization  $N_{q\pi}$  can be deduced from  $N_{q\rho}$  by generalizing the Goldberger-Treiman relation to the  $\rho$ -quark coupling [26]:

$$\frac{g_{\pi qq}^2}{4\pi} = \left(\frac{g_q^A}{g_N^A}\right)^2 \left(\frac{m_q}{m_N}\right)^2 \frac{g_{\pi NN}^2}{4\pi} = \left(\frac{3}{5}\right)^2 \left(\frac{340}{939}\right)^2 14.2 = 0.67 \quad (\text{B3})$$

$$\frac{(g_{\rho qq}^V + g_{\rho qq}^T)^2}{4\pi} = \left(\frac{g_q^A}{g_N^A}\right)^2 \left(\frac{m_q}{m_N}\right)^2 \frac{(g_{\rho NN}^V + g_{\rho NN}^T)^2}{4\pi} = \left(\frac{3}{5}\right)^2 \left(\frac{340}{939}\right)^2 27.755 = 1.31,$$

where  $g_N^A, m_N$  are the nucleon axial coupling constants and mass, respectively, as well as  $g_q^A, m_q$  the quark ones. The  $\pi NN$  coupling is  $g_{\pi NN}^2/4\pi = 14.2$ ; the vector  $\rho NN$  coupling is  $(g_{\rho NN}^V)^2/4\pi = 0.55$  and its ratio to the tensor coupling is  $g_{\rho NN}^T/g_{\rho NN}^V = 6.105$  [27]. From the above relations, we deduce

$$\frac{g_{\pi qq}}{(g_{\rho qq}^V + g_{\rho qq}^T)} \equiv \frac{N_{q\pi}}{N_{q\rho}} = 0.715. \quad (\text{B4})$$

As a final comment, we have explicitly checked that with the above rules the background diagram leads to a cross section that qualitatively shows the same  $s$  dependence of experimental data for  $\pi\pi$  production in the relative  $L=0$  channel when  $s$  is inside the  $\rho$  resonance width, in any case below the first dip corresponding to the resonance  $f_0(980)$  [28]. If we reasonably assume that the resonant diagram exhausts almost all of the  $\pi\pi$  production in the relative  $L=1$  channel and we also assume that in the given energy interval the  $L=0,1$  channels approximate the whole strength for  $\pi\pi$  production, we can safely state that the diagrams of Fig. 4 give a satisfactory reproduction of the  $\pi\pi$  cross section, with invariant mass in the given interval, without invoking any scalar  $\sigma$  resonance (cf. [9,11]).

- 
- [1] R.L. Jaffe, in *Physics with an Electron Polarized Light-Ion Collider: Second Workshop, EPIC 2000*, edited by R. G. Milner, AIP Conf. Proc. No. 588 (AIP, Melville, NY, 2001), p. 54.
- [2] J.P. Ralston and D.E. Soper, Nucl. Phys. **B152**, 109 (1979).
- [3] R.L. Jaffe, hep-ph/9710465.
- [4] O. Martin, A. Schafer, M. Stratmann, and W. Vogelsang, Phys. Rev. D **57**, 3084 (1998).
- [5] J. Collins, Nucl. Phys. **B396**, 161 (1993).
- [6] A. de Rújula, J.M. Kaplan, and E. de Rafael, Nucl. Phys. **B35**, 365 (1971).
- [7] R.L. Jaffe and X. Ji, Phys. Rev. Lett. **71**, 2547 (1993).
- [8] D. Boer and P.J. Mulders, Phys. Rev. D **57**, 5780 (1998).
- [9] J.C. Collins and G.A. Ladinsky, hep-ph/9411444.
- [10] J.C. Collins, S.F. Heppelmann, and G.A. Ladinsky, Nucl. Phys. **B420**, 565 (1994).
- [11] R.L. Jaffe, Xuemin Jin, and Jian Tang, Phys. Rev. Lett. **80**, 1166 (1998).
- [12] A. Bianconi, S. Boffi, R. Jakob, and M. Radici, Phys. Rev. D **62**, 034008 (2000).
- [13] D. Boer, Nucl. Phys. **B603**, 195 (2001); and (private communications).
- [14] HERMES Collaboration, A. Airapetian *et al.*, Phys. Rev. Lett. **84**, 4047 (2000); Phys. Rev. D **64**, 097101 (2001); Spin Muon Collaboration, A. Bravar, Nucl. Phys. B (Proc. Suppl.) **79**, 520 (1999).
- [15] L. Bourhis, M. Fontannaz, J.Ph. Guillet, and M. Werlen, Eur. Phys. J. C **19**, 89 (2001); S. Kretzer, Phys. Rev. D **62**, 054001 (2000); B.A. Kniehl, G. Kramer, and B. Potter, Nucl. Phys. **B582**, 514 (2000).
- [16] H. Meyer and P.J. Mulders, Nucl. Phys. **A528**, 589 (1991); W. Melnitchouk, A.W. Schreiber, and A.W. Thomas, Phys. Rev. D **49**, 1183 (1994); J. Rodrigues, A. Henneman, and P.J. Mulders, nucl-th/9510036.
- [17] R. Jakob, P.J. Mulders, and J. Rodrigues, Nucl. Phys. **A626**, 937 (1997).
- [18] A. Bacchetta, R. Kundu, A. Metz, and P.J. Mulders, Phys. Lett. B **506**, 155 (2001).
- [19] A. Bianconi, S. Boffi, R. Jakob, and M. Radici, Phys. Rev. D **62**, 034009 (2000).
- [20] V. Barone, A. Drago, and P.G. Ratcliffe, Phys. Rep. **359**, 1 (2002).
- [21] D.E. Soper, Phys. Rev. D **15**, 1141 (1977); Phys. Rev. Lett. **43**, 1847 (1979); J.C. Collins and D.E. Soper, Nucl. Phys. **B194**, 445 (1982); R.L. Jaffe, *ibid.* **B229**, 205 (1983).
- [22] M. Glück, E. Reya, and A. Vogt, Eur. Phys. J. C **5**, 461 (1998).
- [23] M. Glück, E. Reya, M. Stratmann, and W. Vogelsang, Phys. Rev. D **53**, 4775 (1996).

- [24] Y. Nambu and J.J. Sakurai, Phys. Rev. Lett. **8**, 79 (1962); **8**, 191(E) (1962); M. Gell-Mann, D. Sharp, and W. Wagner, *ibid.* **8**, 261 (1962).
- [25] B. L. Ioffe, V. A. Khoze, and L. N. Lipatov, *Hard Processes* (Elsevier, Amsterdam, 1984), Vol. 1.
- [26] L.Y. Glozman, Z. Papp, W. Plessas, K. Varga, and R.F. Wagenbrunn, Phys. Rev. C **57**, 3406 (1998); R.F. Wagenbrunn, L.Y. Glozman, W. Plessas, and K. Varga, Nucl. Phys. **A663&664**, 703 (2000).
- [27] T. E. Ericson and W. Weise, *Pions in Nuclei* (Clarendon, Oxford, 1988).
- [28] M.R. Pennington, hep-ph/9905241.